Low-Complexity Quantized Prescribed Performance Control for Constrained Steer-by-Wire Systems with Input Nonlinearity and Bandwidth Limitations

Jiwu Li, Bingxin Ma, Hongjuan Li, and Yongfu Wang

***Abstract*—This paper investigates the low-complexity prescribed performance control problem for uncertain steer-by-wire (SbW) systems subject to input nonlinearity (i.e., actuator fault and dead-zone), full-state constraints, and communication bandwidth limitations. Without the accurate mathematical model and introducing intelligent approximation/parameter estimation techniques, a low-complexity prescribed performance control method is proposed based on a new error transformation and barrier Lyapunov function technique, which utilizes inherent robustness to handle model uncertainty, input nonlinearity, and quantization and event-triggering error. Besides, a dual quantization control scheme is developed to compensate for the effect of discontinuous signals caused by state and input quantization in the closed-loop control system. Finally, theoretical analysis shows that the tracking error and full-state can be constrained to prescribed sets within a presetting time, and the closed-loop stability can be guaranteed. Numerical simulations and experiments are given to verify the validity of the proposed methods.**

***Index Terms*—Steer-by-wire (SbW) system, input nonlinearity, full-state constraints, state and input quantization, prescribed performance control**

I. Introduction

With the progress of industrial electronic information techniques, intelligent automotive techniques have developed rapidly and are gradually being applied. As one of the necessary execution systems in the motion control layer, the Steer-by-Wire (SbW) system has been the research hotspot in the field of intelligent vehicles [1]–[3]. Due to its ability to adjust the front-wheel steering angle of intelligent vehicles in real-time according to the instructions planned by the path planning layer, driving safety can be guaranteed, and traffic efficiency can be improved [4]–[6]. Therefore, the research on SbW systems has attracted widespread attention in academia and industry in recent years.

This work was partly supported by the Science and Technology Project of the Hebei Education Department under Grant QN2023169, the Ningxia Natural Science Foundation of China under Grant 2023AAC03360, and the Ningxia University Research Project under Grant NGY2022147. (*Corresponding author: Bingxin Ma.*)

Jiwu Li is with the School of Vehicle and Energy, Yanshan University, Qinhuangdao, 066004, China (e-mail: ljw4211@stumail.ysu.edu.cn).

Bingxin Ma is with the School of Vehicle and Energy, Yanshan University, and also with the Hebei Key Laboratory of Special Carrier Equipment, Qinhuangdao, 066004, China (e-mail: bingxinma@ysu.edu.cn).

Hongjuan Li is with the School of Mechanical Engineering, Ningxia Institute of Science and Technology, Shizuishan, 753000, China (e-mail: hongjuanli@stumail.neu.edu.cn).

Yonghfu Wang is with the School of Mechanical Engineering and Automation, Northeastern University, Shenyang, 110819, China (e-mail:yfwang@mail.neu.edu.cn).

Significant contributions have been made to the literature on control problems for SbW systems; see, e.g., [3]–[13] and the references therein. Specifically, considering the common model uncertainty of SbW systems caused by unknown parameters and external disturbance, a robust sliding mode control [7]–[9] is designed to ensure tracking performance. To eliminate the effect of actuator and controller-area-network (CAN) communication faults on the control performance, the model predictive control combined with the state observer and adaptive techniques is proposed in [10]–[12]. References [3], [5], [6], [13] construct the fuzzy logic system (FLS)-based and adaptive neural network-based event-triggered controller (ETC) of SbW systems to deal with serious model uncertainty (e.g., unmodeled dynamics), unmeasurable state, and limited communication resources, respectively. The above studies have solved the control problem of SbW systems with model uncertainty, actuator fault, and limited communication resources, and there are still the following practical engineering requirements of the SbW system:

- The existing control methods for dealing with model uncertainty are mainly based on parameter estimation, intelligent approximator and observer techniques, which ignore the burdensome computation and the timeliness problems, such that the practical applicability of the developed controller may be reduced.
- The problem of limited communication bandwidth in the sensor-to-controller and controller-to-actuators channels (i.e., dual quantization) has not been considered, which reduces the practical applicability of the developed controller. Besides, the full-state constraints phenomenon for SbW systems (i.e., the steering angle and steering angular velocity of the front wheels) has not been considered.

Thus, considering the problems outlined above, how to construct an effective control method for uncertain SbW systems with full-state constraints and limited communication bandwidth is worthy of further study.

Recently, many significant achievements have been developed for prescribed tracking control of nonlinear systems; see, e.g., [14]–[29] and the references therein. Representatively, for the nonlinear system with model uncertainty, a prescribed performance control method based on the parameter adaptation and approximator technologies is presented in [14]–[16], respectively. To address input nonlinearity and state constraints, references [17]–[20] and references [21]–[23]

develop the prescribed performance controllers for nonlinear systems. Considering the model uncertainties and time-varying delays, the low-complexity prescribed performance control method is developed for nonlinear systems in [27]–[29]. Besides, the prescribed performance controller is proposed in [24]–[26] for uncertain nonlinear systems with input quantization and unknown measurement sensitivity by combining the backstepping method. Although the above research on the prescribed tracking control problem of nonlinear systems has made significant contributions, the limited communication bandwidth in the sensor-to-controller channel has not yet been considered in existing research. Therefore, the prescribed performance control problem of nonlinear SbW systems with limited communication bandwidth is worthy of further study.

Motivated by the aforementioned discussions, this paper studies the prescribed tracking control problem of quantization for uncertain SbW systems with input nonlinearity (i.e., actuator fault and dead-zone), full-state constraints, low-complexity, and the limitations of communication bandwidth and resources. Without utilizing approximation/adaptive techniques and prior knowledge regarding the model nonlinearity of controlled plants, a low-complexity prescribed performance control method for SbW systems is proposed by introducing a new error transformation and barrier Lyapunov function technique. The state and input quantization are utilized to actively reduce the communication bandwidth of the SbW system. The inherent robustness of the developed method can counteract model uncertainty, input nonlinearity, and quantization errors. Furthermore, an event-triggering mechanism (ETM) is also introduced to save communication resources. Theoretical analysis, simulations, and experiments are given to verify the effectiveness of the proposed method. The contributions of this study can be summarized as:

- Compared with the control research of SbW systems [3]–[13]: (i) a low-complexity prescribed performance control is proposed in this paper, without introducing the parameter estimation, intelligent approximator and observer techniques, such that the burdensome computation and the timeliness problems can be solved; (ii) the effect of limited communication bandwidth on the control performance is considered in this paper, which improved the practical applicability of the developed controller.
- Compared with the prescribed performance control research of nonlinear systems [14]–[29], the inevitable phenomena of nonlinear SbW systems, including the limited communication bandwidth in the sensor-to-controller channel, are considered. As a result, the prescribed performance controller developed in this paper can achieve better practical industrial applications.

The rest of this paper is organized as follows: Section II presents the dynamic model of the SbW system, quantizer design, and control objectives. The control design and system stability analysis are given in Section III. Section IV provides simulations and experiments. Finally, the concluding remark is given in Section V.

II. Problem Formulation

A. Dynamics model

The schematic diagram of SbW systems is shown in Fig. 1 [4]. According to existing research [6], the dynamic model of SbW systems can be expressed as

$$\mathcal{J}_e\ddot{\theta}_f + \mu^2\mathcal{B}_m\dot{\theta}_f + \mathcal{H}_f(\theta_f,\dot{\theta}_f) = \mu(\tau_m(t) + \tau_d(t)) \quad (1)$$

where $\mathcal{J}_e = \mathcal{J}_f + \mu^2\mathcal{J}_m$ is the equivalent moment of inertia with $\mathcal{J}_f$ and $\mathcal{J}_m$ being the rotational inertia of the front wheel and steering motor, $\mathcal{H}_f(\theta_f,\dot{\theta}_f) = \tau_e(x) + \tau_f(x)$ denotes the uncertain nonlinearity including the self-aligning torque and friction torque of the front wheel, θ_f denotes the steering angle of the front wheel, μ and $\mathcal{B}_m$ are the ratio of motor output shaft angle to front wheels angle and the viscous friction coefficient of the motor, respectively. $\tau_m(t)$ and $\tau_d(t)$ are the output torque of steering motor assembly and the motor torque pulsation disturbance [6].

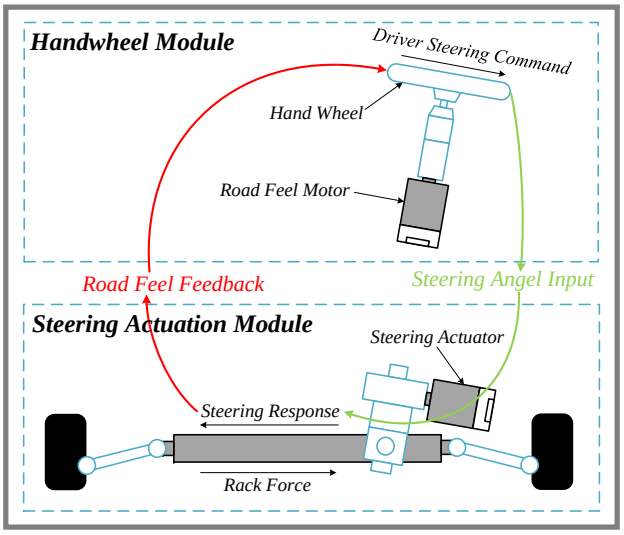

Fig. 1. Schematic diagram of SbW systems.

Note that this paper further considers the input nonlinearity problem of the SbW system, including actuator fault caused by electromagnetic interference and dead-zone phenomenon caused by gear backlash in the transmission system between the steering motor and the front wheels. The output torque of the steering motor is described as

$$\tau_m(t) = \ell(t)\tau_c^* + \varsigma(t) \quad (2)$$

with τ_c^* being the control signal formed by the controller, $\tau_m(t)$ being the output of the steering motor, and $\ell(t) > 0$ and $\varsigma(t)$ being unknown time-varying parameters.

Combined with (1)-(2), the mathematical model of SbW systems with actuator fault and dead-zone phenomenon can be expressed as

$$\begin{cases} \dot{x}_1 = x_2 \\ \dot{x}_2 = f(x) + g(t)\ell(t)u + d(t) \\ y = x_1 \end{cases} \quad (3)$$

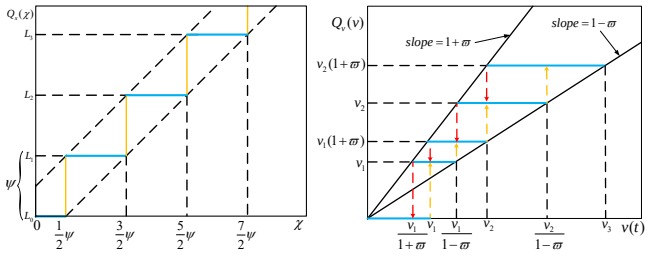

(a) Uniform quantizer (b) Hysteresis quantizer

Fig. 2. Quantizer schematic diagram.

where $x = [x_1, x_2]^T = [\theta_f, \dot{\theta}_f]^T \in \mathbb{R}^2$ is the state of the SbW system, $u = \tau_c^* \in \mathbb{R}$ is the control signal, $y \in \mathbb{R}$ denotes the output of SbW systems, $f(x) = -(\mu^2 \mathcal{B}_m x_2 + \mathcal{H}_f(x))/\mathcal{J}_e : \mathbb{R}^2 \to \mathbb{R}$ represents the uncertain lumped nonlinearity including the friction torque τ_f and self-aligning torque τ_e, $g(t) = \mu/\mathcal{J}_e \in \mathbb{R}$ is the uncertain control coefficient, and $d(t) = \mu\tau_{d\varsigma}(t)/\mathcal{J}_e$ is considered as the disturbance. The detailed parameter definitions can be found in Tab. I.

Remark 1: For the uncertain lumped nonlinearity $f(x)$ of the SbW system: (i) Although the parameter uncertainty of SbW systems is considered in existing research [7], [30], e.g., $\tau_e = -C_f(t_p + t_m)(\beta + \frac{\gamma l_f}{v} - x_1)$ and $F_f^y = -C_f \alpha_f$, detailed parameters can be found in [7], these references are based on the assumption that the cornering stiffness coefficient C_f and the mechanical and pneumatic trail t_p, t_m, have upper bounds, and at a small slip angle such as 4° or less, the lateral force F_f^y is considered to be linearly correlated with the tire slip angle α_f, which is not applicable in some practical working conditions. (ii) Besides, based on intelligent approximation/parameter estimation techniques, the fuzzy logic system is introduced in existing references [3], [5], [6] to approximate $f(x)$. However, the FLS technique increases the computational load of the automotive electronic control unit (ECU) and cannot approximate the discontinuous coulomb friction and viscous friction models, which is not suitable for practical engineering applications.

B. Quantizer Design

The quantization problem of the SbW system in this paper is considered to save the communication bandwidth and energy consumption of signals during CAN transmission of state and control input. In state quantization, a uniform quantizer [31] is utilized and modeled as

$$Q_x(\chi) = \begin{cases} L_i, & Case\ I: L_i - \psi/2 \le \chi(t) < L_i + \psi/2 \\ 0, & Case\ II: -\psi/2 \le \chi(t) < \psi/2 \\ -L_i, & Case\ III: -L_i - \psi/2 \le \chi(t) < -L_i + \psi/2 \end{cases} \tag{4}$$

where $\chi(t) = \lambda x_1(t) + x_2$ and $L_0 = 0$, $L_{i+1} = L_i + \psi$ $(i = 0, 1, 2, ...,$ i.e., $L_1 = \psi$, $L_2 = 2\psi$, $L_3 = 3\psi, ...)$, $\psi > 0$ is the length of the quantization interval. $Q_x(\chi)$ is in the set $U = \{0, \pm L_i\}$ and $|\chi(t) - Q_x(\chi)| \le \psi/2$. The map of the uniform quantizer $Q_x(\chi)$ for $\chi > 0$ is shown in Fig. 2(a).

The continuous control input signal is quantified through a hysteretic quantizer in [32], which is modeled as

$$Q_v(v) = \begin{cases} v_i, & Case\ I: \frac{v_i}{1+\varpi} < v \le v_i, Q_v^- \ge v_i \\ & or\ v_i \le v < \frac{v_i}{1-\varpi}, Q_v^- \le v_i \\ v_i(1+\varpi), & Case\ II: v_i \le v \le \frac{v_i}{1-\varpi}, Q_v^- \ge v_i(1+ \\ & \varpi) or \frac{v_i}{1-\varpi} \le v < v_i,\ Q_v^- \le v_i(1+\varpi) \\ 0, & Case\ III: 0 \le v \le \frac{v_i}{1+\varpi}, Q_v^- \ge v_i(1+ \\ & \varpi)\ or\ \frac{v_i}{1+\varpi} < v < v_1, Q_v^- = 0 \\ -Q_v(-v), & Case\ IV: v < 0. \end{cases} \tag{5}$$

where $v_i = \beta^{1-i} v_{min}$ $(i = 1, ..., n)$, i represents the number of terms, and $v_{min} > 0$ stands for the dead-zone size of $Q_v(v)$ with parameter $\varpi = (1-\beta)/(1+\beta)$, $0 < \beta < 1$. The constant term β denotes the density of quantization, and the smaller β is, the coarser the quantization controller is. $Q_v^-(t)$ is the latest value of $Q_v(v)$ before the time instant t, and $Q_v^-(0) = 0$. The map of the hysteresis quantizer $Q_v(v)$ for $v(t) > 0$ is shown in Fig. 2(b).

Remark 2: (i) Considering that the quantization error $l/2$ of the uniform quantizer is bounded and can be designed, the uniform quantizer is used to quantify the system state. Considering the discontinuity of the quantified state, the hysteresis quantizer is used for input quantization to reduce controller output chattering. (ii) The quantization is inevitable owing to the high-precision sensors and digital processors in SbW systems are contradictory to the limited communication bandwidth, and signal loss phenomenon may occur during signal transmission, i.e., there is an error between the signal in the channel and the measurement signal. Fig. 2(a) and (b) show that quantization is a kind of mapping from continuous signals to discrete finite sets, thereby reducing the burden of signal transmission and the effect of signal loss caused by limited channel bandwidth.

Lemma 1 [32]: The hysteresis quantizer (5) can be decomposed as follows:

$$Q_v(v) = \alpha(v)v(t) + \gamma(v) \tag{6}$$

with $\alpha(v)$ and $\gamma(v)$ being defined as

$$\alpha(v) = \begin{cases} \frac{Q_v(v)}{v}, & Q_v(v) \ne 0 \\ 1, & Q_v(v) = 0 \end{cases}, \gamma(v) = \begin{cases} 0, & Q_v(v) \ne 0 \\ -v, & Q_v(v) = 0 \end{cases}.$$

Moreover, in the decomposition (6), $\alpha(v)$ and $\gamma(v)$ satisfy the following condition:

$$1 - \varpi \le \alpha(v) \le 1 + \varpi, \quad |\gamma(v)| \le v_{min}. \tag{7}$$

A lemma is first given to support the stability analysis of the closed-loop system.

Lemma 2: If the bounds of $z(t)$ and $x_1(0)$ are known, i.e., $|z(t)| \le \rho(t)$ and $|x_1(0)| \le \sigma$ with σ being an unknown

TABLE I
NOMENCLATURE

Notations	Descriptions
In the SbW system	
$\mathcal{J}_f$	Rotational inertia of the front wheel
$\mathcal{J}_m$	Rotational inertia of the steering motor
$\mathcal{J}_e$	Equivalent moment of inertia
τ_e	Self-aligning torque of the front wheel
τ_d	Motor torque pulsation disturbance
τ_f	Friction torque of the front wheel
$\mathcal{H}_f$	Uncertain nonlinearity of the SbW system
θ_f	Steering angle of front wheels
μ	Ratio of motor output shaft angle to front wheels angle
$\mathcal{B}_m$	Viscous friction coefficient of the motor
τ_m	Output torque of steering motor assembly
τ_c^*	Control signal formed by the controller
$\ell(t)$, $\varsigma(t)$	Unknown time-varying parameters
In the state space equation	
x	State of the SbW system
$u = \tau_c^*$	Control signal
y	Output of the SbW system
$f(x)$	Uncertain lumped nonlinearity
$g(t)$	Uncertain control coefficient
$d(t)$	Disturbance of the SbW system
In the state and input quantizer	
$\chi(t)$	Input of the state quantizer
$Q_x(\chi)$	Output of the state quantizer
ψ	Length of the state quantizer interval
v	Input of the input quantizer
$Q_v(v)$	Output of the input quantizer
v_{min}	Dead-zone size of $Q_v(v)$
β	Density of the input quantizer
$Q_v^-(t)$	Latest value of $Q_v(v)$ before the time instant t,
In the controller	
z	Error transformation
$v(t)$	Control law and input of the input quantizer
$\rho(t)$	Prescribed performance function
η, λ, ξ_0, ξ_1, t_ξ, ϱ, m, κ	Positive constant to be designed
$Q_v(v(t)_k)$	Input of the ETM
$u(t)$	Output of the ETM and control signal

positive constant, the tracking error and full-state of SbW systems are prescribed, i.e.,

$$\rho_0^l \le x_1 - y_d \le \rho_0^r, \quad \rho_i^l \le x_i \le \rho_i^r, \quad i = 1, 2 \tag{8}$$

where $\rho_j^l(t)$, $\rho_j^r(t)$, $j = 0, 1, 2$, and the definition of parameters and the theoretical proof are provided in *Appendix A*.

The assumptions about the desired steering angle of front wheels and input nonlinearity are given as follows:

Assumption 1: The desired signal $y_d(t)$ and its time derivative $\dot{y}_d(t)$ are bounded and differentiable.

Assumption 2: There exist unknown positive constants $\bar{D}$ and $\underline{\ell}$, such that $d(t) \le \bar{D}$ and $\underline{\ell} < \ell(t)$.

Remark 3: The assumptions mentioned above are quite common. To be specific: (i) For the same assumption on the desired signal $y_d(t)$, Assumption 1 is commonly utilized in the research of the control method of SbW systems [4], [30], [33]. (ii) For the input nonlinearity of SbW systems, Assumption 2 of this paper is commonly utilized in current research; see [3] and the references therein. Thus, Assumptions 1-2 used in this paper are common.

C. Control Objective

The main purpose of this paper is to design a low-complexity prescribed performance control for SbW systems with state and input quantization such that: (i) The tracking error of SbW systems can converge to the prescribed neighborhood of the origin in the presence of the state and input quantization, input nonlinearity, and model uncertainty. (ii) After the state and input are quantified, the CAN communication resources can be further saved through ETM, while the Zeno behavior can be avoided. (iii) All the signals of the resulting closed-loop system remain locally uniformly ultimately boundedly.

Remark 4: The control objectives of SbW systems mentioned above are reasonable in practice. Specifically: (i) To improve driving safety, the prescribed performance of the tracking performance of SbW systems should be considered in the controller design. (ii) To reduce the state and control input signals effect of communication bandwidth limitation in the process of CAN transmission, state and input quantization should be considered. (iii) To save the communication volume of the SbW system and ensure other applications of the vehicle to obtain more communication resources, the event-triggering mechanism between the controller and the actuator is considered. (iv) To ensure the stability of closed-loop systems and prevent storage overflow of the controller, all signals of the closed-loop system must be globally uniformly bounded. Therefore, the practical control requirements of SbW systems mentioned above are considered in the control objectives.

III. Control Design and Main Results

A. Control Design

The following error transformation is given as

$$z = \chi(t) - \lambda y_d \tag{9}$$

where $\chi(t) = \lambda x_1 + x_2$, x_1 and x_2 refer to θ_f and $\dot{\theta}_f$, respectively, and λ is the positive constant to be designed. After being quantified by the smart sensors, $\chi(t) = Q_x(\chi)$. The control law $v(t)$ is designed as

$$v(t) = -\eta S(z(t)), \quad S(z(t)) = \tan\left(\frac{\pi}{2}\frac{z(t)}{\rho(t)}\right) \tag{10}$$

where η is the positive constant to be designed, and the prescribed performance function $\rho(t)$ is

$$\rho(t) = \begin{cases} \xi_1 + (\xi_0 - \xi_1)e^{\left(-\frac{t}{t_\xi - t}\right)}, & Case\ I{:}\ 0 \le t < t_\xi \\ \xi_1, & Case\ II{:}\ otherwise \end{cases} \tag{11}$$

where ξ_0 and ξ_1 are positive constants to be designed, and t_ξ is the presetting time. The control signal $u(t)$ of SbW systems

and the ETM utilized to save communication resources in the controller-to-actuator channel are constructed as

$$u(t) = Q_v(v(t_k)) \quad \forall t \in [t_k, t_{k+1}),\ t_1 = 0 \tag{12}$$

$$t_{k+1} = \begin{cases} inf\{t > t_k : |e_v(t)| \geq \varrho |v(t)| + m\}, \\ \qquad\qquad Case\ I\text{: } if\ |v(t)| \leq \kappa \\ inf\{t > t_k : |e_v(t)| \geq m\}, Case\ II\text{: } otherwise \end{cases} \tag{13}$$

where ϱ, $0 \leq \varrho < 1$, $\kappa > 0$, $m > 0$ and $e_v(t) = u(t) - Q_v(v(t))$. If the condition (13) is met at time t_k, then $u(t) = Q_v(v(t_k))$, $t \in [t_k, t_{k+1})$, and t_{k+1} is the next triggering time. The designed quantification and event-triggered control system are shown in Fig.3, and the detailed parameter definitions can be found in Tab. I.

Remark 5: Note that this paper mainly considers the effect of the communication bandwidth of SbW systems control, including the communication bandwidth from sensor to controller and controller to actuator. The state quantizer (4) is utilized in the smart sensor, so the signal sent from the sensor to the controller is quantized and discontinuous. The input quantizer (5) is utilized in the controller, and $v(t)$ is utilized as a control law to output to the actuator through the input quantizer (5) and ETM (12)-(13). See Fig.3.

Remark 6: The developed controller (5) and (9)-(13) for the SbW system in this paper has the following advantages: (i) Compared with traditional controllers such as PID and sliding mode control [6], [30], prescribed performance control has the advantage that the controlled error can converge to the prescribed residual set $\rho_0^l \leq x_1 - y_d \leq \rho_0^r$ within a presetting time t_ξ, which can improve the control performance of steering track. (ii) Compared with other prescribed performance controls [3], [5], this paper proposes a novel control law $v(t)$ construction method to robust the effect of uncertain lumped nonlinearity $f(x)$ and the model parameters in SbW system, so there is no need for intelligent approximation/parameter estimation techniques such as FLS, which can reduce the complexity of the controller and improve the operational efficiency of the ECU. Besides, the limitations of communication bandwidth and resources are considered, and the input quantizer and ETM are designed in the controller. (iii) From *Lemma 2*, *Appendix A*, and (9), it can be seen that a new error transformation is constructed so that the prescribed tracking performance control is guaranteed, and more importantly, the problem of full-state constraints of the SbW system is solved.

B. Main Results

Based on the quantification (4)-(5) and event-triggering mechanism (12)-(13), the time derivative of S can be expressed as

$$\dot{S} = \frac{\pi}{2\rho^2 cos^2\left(\frac{\pi}{2}\frac{z(t)}{\rho(t)}\right)}(\rho(t)(f(x) + g\ell(t)u(t) + d(t) + \lambda x_2 - \lambda \dot{y}_d(t)) - \dot{\rho}(t)z(t)). \tag{14}$$

For the SbW system (3) with the developed control schemes (9)-(13) and state and input quantizer (4)-(5), the main results can be summarized in the following theorem.

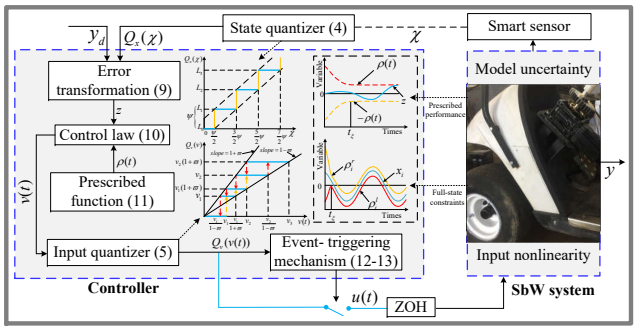

Fig. 3. Block diagram of the proposed control scheme.

Theorem 1: Consider the SbW system (3) with model uncertainty, input nonlinearity (2), the quantizers (4)-(5), and ETM in the controller-to-actuator channel (12)-(13). Under Assumptions 1-2 hold, the control objective can be guaranteed by the developed control schemes (9)-(10) with the condition $|z(0)| < \rho(0)$, and all signals in the closed-loop system are guaranteed to be bounded.

Proof: Consider the barrier Lyapunov function is

$$V = \frac{1}{2}S^2(t). \tag{15}$$

The time derivative of V is computed based on (14) as

$$\dot{V} = \frac{S\pi}{2\rho^2 cos^2\left(\frac{\pi}{2}\frac{z(t)}{\rho(t)}\right)}(\rho(t)(f(x) + g\ell(t)u(t) + d(t) + \lambda x_2 - \lambda \dot{y}_d(t)) - \dot{\rho}(t)z(t)). \tag{16}$$

From (13), one gets that there exist $|o_i(t)| < 1, i = 1, 2$, such that $Q_v(v(t)) = (1 + o_1(t)\rho_1)u(t) + o_2(t)m$. The relationship between $Q_v(v(t))$ and $u(t)$ can be expressed as

$$u(t) = \frac{Q_v(v(t))}{1 + o_1(t)\rho_1} - \frac{o_2(t)m}{1 + o_1(t)\rho_1}. \tag{17}$$

Substituting (17) to (16) yields

$$\dot{V} = \frac{S\pi}{2\rho^2 cos^2\left(\frac{\pi}{2}\frac{z(t)}{\rho(t)}\right)}(\rho(t)(f(x) + go'(t)Q_v(v(t)) + d_1'(t) + \lambda x_2 - \lambda \dot{y}_d(t)) - \dot{\rho}(t)z(t)). \tag{18}$$

with $o'(t) = \frac{\ell(t)}{1 + o_1(t)\rho_1}$ and $d_1'(t) = d(t) - go'(t)o_2(t)m$.

From (5) and *Lemma 1*, one gets that $Q_v(v(t)) = \alpha(v)v(t) + \gamma(v)$. Thus, substituting (6) to (18) yields

$$\dot{V} = \frac{S\pi}{2\rho^2 cos^2\left(\frac{\pi}{2}\frac{z(t)}{\rho(t)}\right)}(\rho(t)(f(x) + g\ell'(t)v(t) + d_2'(t) + \lambda x_2 - \lambda \dot{y}_d(t)) - \dot{\rho}(t)z(t)). \tag{19}$$

with $\ell'(t) = o'(t)\alpha(u)$ and $d_2'(t) = d_1'(t) + go'(t)\gamma(u)$.

Combined with the definition of $z(t)$ and state quantizer (4), one gets that

$$|\chi(t) - Q_x(\chi)| \leq \psi/2,\ and\ |z + \lambda y_d - Q_x(\chi)| \leq \psi/2. \tag{20}$$

Combining (20), it can be concluded that there exists a variable $o_3(t), |o_3(t)| \leq 1$, such that

$$z(t) = Q_x(\chi) + \frac{\psi}{2} o_3(t) - \lambda y_d. \tag{21}$$

The following is an analysis of the worst-case dynamics of $S(t)$, i.e., $\rho(t) - \frac{\psi}{2} \leq |Q_x(\chi) - \lambda y_d| \leq |z(t)| \leq \rho(t)$, where $\psi/2$ is the maximum quantization error of the state quantizer (see, for instance, Fig.4), which can be derived as $sign(z) = sign(Q_x(\chi) - \lambda y_d)$.

Remark 7: Here is a detailed explanation of the above analysis and Fig. 4: (i) $\psi/2$ refers to the quantization error of the state quantizer. When $|Q_x(\chi) - \lambda y_d| < \rho(t) - \psi/2$, according to (21), $z(t)$ is within the prescribed range, i.e., $-\rho(t) < z(t) < \rho(t)$. (ii) As $z(t)$ is a continuous function, when $|z(t)| \geq |Q_x(\chi) - \lambda y_d| \geq \rho(t) - \psi/2$, $z(t)$ may approach the prescribed boundary $\rho(t)$, which is the worst-case dynamics of $S(t)$. (iii) This paper proves that when the worst-case dynamics occur, the control system is stable and the $z(t)$ of SbW systems will not exceed the prescribed boundary $\rho(t)$.

The above analysis concludes that there exists a positive time-varying variable $o_4(t), \underline{o}_4 \leq o_4(t) < 1$, with $\underline{o}_4$ being an unknown positive constant, such that

$$\tan\left(\frac{\pi}{2}\frac{Q_x(\chi) - \lambda y_d}{\rho(t)}\right) = o_4(t)\tan\left(\frac{\pi}{2}\frac{z(t)}{\rho(t)}\right). \tag{22}$$

Substituting (22) into (19) yields

$$\begin{aligned}\dot{V} =& \frac{S\pi}{2\rho^2 cos^2\left(\frac{\pi}{2}\frac{z(t)}{\rho(t)}\right)}(\rho(t)(f(x) - g\eta\ell^{'}(t)o_4(t)S(z(t)) \\ &+ d_2^{'}(t) + \lambda x_2 - \lambda\dot{y}_d(t)) - \dot{\rho}(t)z(t)).\end{aligned} \tag{23}$$

Then, the following conditions are given to analyze the dynamic behavior of V: (i) From *Lemma 2*, it can be concluded that $x_i, i = 1, 2$ is bounded, and $f(x)$ and g are also bounded. (ii) Combined with the Assumption 2 and (17)-(22), one can get that $\ell^{'}(t)$ and $d_2^{'}(t)$ are bounded, and $g\ell^{'}(t)o_4(t) > 0$. (iii) From (11), bounded $\rho(t)$ and $\dot{\rho}(t)$ can be obtained.

From the above analysis, it can be seen that there exists an unknown positive constant $\bar{\Gamma}$ such that

$$\bar{\Gamma} \geq |\rho(t)f(x) + \rho(t)d_2^{'}(t) + \lambda\rho(t)x_2 - \lambda\rho(t)\dot{y}_d(t) - \dot{\rho}(t)z(t))|.$$

Substituting the above inequality into (23), one gets

$$\dot{V} \leq \frac{|S|\pi}{2\rho^2 cos^2\left(\frac{\pi}{2}\frac{z(t)}{\rho}\right)}\left(\bar{\Gamma} - \rho(t)g\eta\ell^{'}(t)o_4(t)|S|\right). \tag{24}$$

From (24), one can obtain that there exists an unknown positive constant Θ, $|S| = \Theta$ for $t = t_\Theta$ such that

$$\dot{V}|_{t=t_\Theta} \leq 0, \quad if \quad \Theta \geq max\left\{|S(z(0))|, \frac{\bar{\Gamma}}{\rho(t)g\eta\ell^{'}(t)o_4(t)}\right\}.$$

Based on the above inequality, one gets that V is bounded, i.e., $V \leq \frac{1}{2}\Theta^2$. Taking the inverse of the S-function, one has

$$-\rho(t) < S^{-1}(-\Theta) \leq z(t) \leq S^{-1}(\Theta) < \rho(t). \tag{25}$$

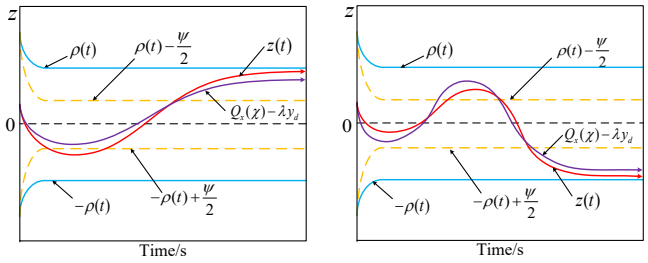

(a) The case that $\rho(t) - \frac{\psi}{2} \leq Q_x(\chi) - \lambda y_d \leq z(t) \leq \rho(t)$

(b) The case that $-\rho(t) \leq z(t) \leq Q_x(\chi) - \lambda y_d \leq -\rho(t) + \frac{\psi}{2}$

Fig. 4. The worst-case dynamics of $z(t)$ are considered in this paper.

The above result (25), with the conclusion of *Lemma 2*, implies that the tracking error of the SbW system (3) can converge to the prescribed neighborhood of the origin. Besides, the above analysis means that all closed-loop signals remain bounded.

Then, the following analysis is given to show that the Zeno behavior, where an infinite number of events occur in a finite-time interval, can be avoided in the designed event-triggered communication. If the Zeno behavior exists, one has $\Delta t = t_{k+1} - t_k = 0$, $k \in Z^+$. This together with (13) yields that $\lim_{\Delta t \longrightarrow 0} |e_v(t_k + \Delta t)| = \lim_{\Delta t \longrightarrow 0} |u(t_k + \Delta t) - Q_v(t_k)| = 0 < m$, which contradicts the ETM (13). Thus, the Zeno behavior does not occur.

This ends the proof of *Theorem 1*. ■

IV. SIMULATION AND EXPERIMENT

A. Simulation parameters selection

1) The SbW system parameters selection: The specific simulation model of SbW systems can be found in [6]. The parameters of (1) are chosen as $\mathcal{J}_f = 3.8\text{kg}\cdot\text{m}^2$, $\mathcal{J}_m = 0.0045\text{kg}\cdot\text{m}^2$, $\mu = 18$ and $\mathcal{B}_m = 0.018\cdot\text{s/rad}$. $\mathcal{H}_f(\theta_f, \dot{\theta}_f) = \tau_e + \tau_f$, in which the friction torque τ_f is considered as [6], i.e., $\tau_f = 0.25(tanh(100x_2) - tanh(x_2)) + 30tanh(100x_2) + 10x_2$, the self-aligning torque τ_e is considered as *Appendix B*, the drive torque $T_{fi} = 50N\cdot m$, $i = r, l$, the initial vehicle speed and wheel rotation speed are $v_x = 19\ m/s$ and $\omega = 57\ rad/s$, respectively, the mechanical and pneumatic trail $t_p = 0.023$, $t_m = 0.016$, and the other parameters are given in [34]. The input nonlinearity of (2) are chosen as $\ell(t) = \ell_f\ell_r$ for $u(t) \geq -\varsigma_l$; $\ell(t) = \ell_f\ell_l$ for $u(t) < -\varsigma_l$, $\varsigma(t) = \varsigma_f(t) - \ell_f\ell_r\varsigma_r$ for $u(t) > \varsigma_r$; $\varsigma(t) = \varsigma_f(t) - \ell_f\ell_r u(t)$ for $-\varsigma_l \leq u(t) \leq \varsigma_r$; $\varsigma(t) = \varsigma_f(t) + \ell_f\ell_l\varsigma_l$ for $u(t) < -\varsigma_l$, where $\ell_l = 1.2$, $\ell_r = 1.4$, $\varsigma_l = 40$ and $\varsigma_r = 30$, and $\ell_f = 1$, $\varsigma_f(t) = 0$ for $t \in [0, 5)s$; $\ell_f = 0.75$, $\varsigma_f(t) = 3sin(4t)$ for $t \in [5, 10)s$; $\ell_f = 0.5$, $\varsigma_f(t) = 4sin(3t)$ for $t \in [10, 15)s$; $\ell_f = 0.25$, $\varsigma_f(t) = 3sin(4t)$ for $t \in [15, 20]s$. Besides, the disturbance is assumed as $d(t) = 5\int[d_m - d(t) + 2rand(1)]dt$ with $d_m = 2cos(6t)$ for $t \in [0, 5)$; $d_m = 2.5cos(4t)$ for $t \in [5, 10)$; $d_m = 3cos(4t)$ for $t \in [10, 15)$; $d_m = 3.5cos(4t)$ for $t \in [15, 20]$.

2) Controller parameters selection: The prescribed performance control design (9)-(13) in simulation, the positive constants $\lambda = 60$, $\eta = 50$, $\xi_0 = 10$, $\xi_1 = 0.09$, and the

TABLE II
SIMULATION PROCESS AND PARAMETER CALCULATION

Step	Calculate
State quantizer (4): $x_1 \longrightarrow Q_x(\chi)$	
Step 1	Input of state quantizer: $\chi = 60x_1 + \dot{x}_1$
Step 2	Case I: $Q_x(\chi) = L_i$, Case III: $Q_x(\chi) = 0$, Case III: $Q_x(\chi) = -L_i$
Case I-III	Please see (4), and $\lambda = 60$, $\psi = 0.01$.
Computational control law (9)-(11): $Q_x(\chi) \longrightarrow v(t)$	
Step 3	Error transformation: $z = Q_x(\chi) - 60y_d$
Step 4	Prescribed performance function: Case I: $\rho(t) = 0.08 + (7 - 0.08)exp(-t/(0.1 - t))$, Case II: $\rho(t) = 0.08$
Step 5	Control law: $v(t) = -100\tan((\pi z(t))/(2\rho(t)))$
Case I-II, and y_d	Please see (11) and *Controller parameters selection.*
Input quantizer (5): $v(t) \longrightarrow Q_v(v)$	
Step 6	Case I: $Q_v(v) = v_i$, Case II: $Q_v(v) = v_i(1 + \varpi)$, Case III: $Q_v(v) = 0$, Case IV: $Q_v(v) = -Q_v(-v)$
Case I-IV	Please see (5), and $\beta = 0.8$, $v_{min} = 0.02$.
ETM (12)-(13): $Q_v(v) \longrightarrow u(t)$	
Step 7	Case I: $u(t) = Q_v(v(t_k))$, Case II: $u(t) = Q_v(v(t_k))$
Case I-II	Please see (12)-(13), and $\varrho = 0.04$, $m = 4$, $\kappa = 10$.
The SbW system (3): $u(t) \longrightarrow x_1$	
Step 8	$\mathcal{H}_f(x) = \tau_e + \tau_f$
Step 9	$\mathcal{J}_e = 3.8 + 18^2 \times 0.0045$
Step 10	$f(x) = -(18^2 \times 0.018x_2 + \mathcal{H}_f(x))/\mathcal{J}_e$
Step 11	$g(t) = 18/\mathcal{J}_e$
Step 12	$d(t) = 5\int[d_m - d(t) + 2rand(1)]dt$
Step 13	$\ddot{x}_1 = \dot{x}_2 = f(x) + g(t)\ell(t)u(t) + d(t)$
τ_e, τ_f, d_m, $\ell(t)$, $\varsigma(t)$	Please see *The SbW system parameters selection.*

preseted steady-state time $t_\xi = 0.2$. Finally, the parameters of the event-triggering mechanism are designed as $\varrho = 0.04$, $m = 4$, and $\kappa = 10$. Besides, the desired signal is selected as $y_d = 0.3sin(0.3t)\ rad$, with an initial value of $x = [0.1, 0]^T$.

3) State quantizer and input quantizer parameters selection: The parameters of state quantizer (4) are selected as $\lambda = 60$ and $\psi = 0.01$. Besides, the parameters of the input quantizer (5) are selected as $\beta = 0.8$ and $v_{min} = 0.2$ in different simulations. The detailed simulation process and parameter calculation are shown in Tab. II.

4) Controller being compared: To verify the effectiveness and low-complexity of the controller proposed in this paper, we choose the existing event-triggered FLS-based control method [3] designed for uncertain SbW systems with input nonlinearity and prescribed performance for comparison. In the simulation, the parameters of [3] are selected as $\eta_1 = 35$, $\eta_2 = 35$, $\delta = 0.5$, $m = 0.01$, and other parameters can be found in [3]. Note that the prescribed boundaries of z_1 in [3] is the same as the new controller, and [3] does not consider the communication bandwidth problem of the SbW systems.

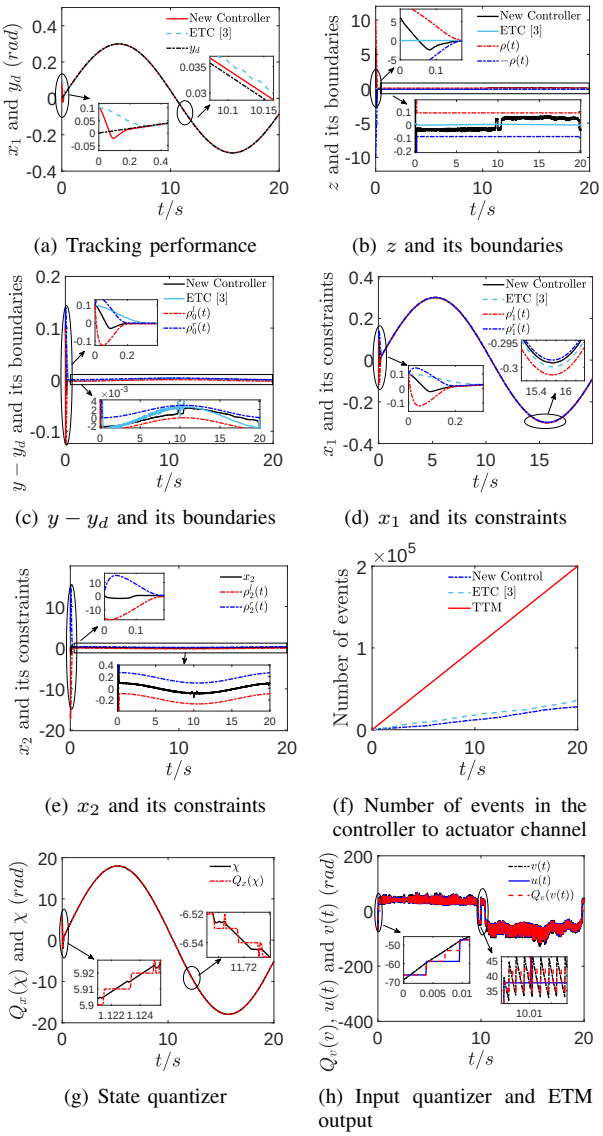

Fig. 5. Comparing simulation and control performance.

B. Simulation results and analysis

Fig.5 gives the comparing simulation and control performance of SbW systems. From Fig.5(a), one can find that the desired signal can be tracked by the output of the SbW system. Fig.5(b) gives the prescribed performance of z under the same boundary for ETM [3] and new controller, Fig.5(c) shows the tracking error between the steering angle y and its desired signal y_d, Fig.5(d)-(e) give that the states x_1 and x_2 of the SbW system are always bounded and can be constrained to the prescribed ranges for new controller, respectively, and Fig.5(f) shows the number of events. From Fig.5(c)-(f), it can be seen that under the same number of events, the error jitter of ETC [3] is more severe than that of the new controller (especially in the 10s), one of the main reasons is that x_2 is constrained within the presetting range in the new controller. Fig.5(g)-(h) show the results of quantifying the state and input. Moreover, Fig.6 and Tab. III give some indicators of tracking

TABLE III
TRACKING PERFORMANCE IN SIMULATIONS

	Indicator	$[0,5)s$	$[5,10)s$	$[10,15)s$	$[15,20]s$
New Controller	IAE	0.0136	0.0028	0.0092	0.0028
	RMSE	0.0081	0.0007	0.0019	0.0007
	SD	0.0080	0.0006	0.0004	0.0007
ETC [3]	IAE	0.0232	0.0073	0.0099	0.0062
	RMSE	0.0146	0.0017	0.0021	0.0015
	SD	0.0145	0.0009	0.0006	0.0010

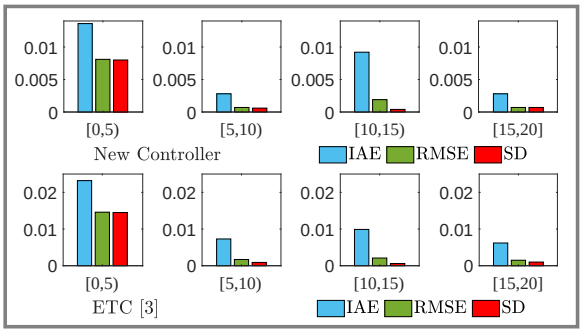

Fig. 6. Indicators of tracking error in simulations.

error, e.g., Integral Absolute Error (IAE), Root Mean Square Error (RMSE), and Standard Deviation (SD) [3].

Remark 8: (i) The parameters in the state quantization comparison are selected as $\eta=90$, $\xi_0=70$, $\xi_0=10$, $\lambda=600$, $\beta=0.5$, $\varrho=0.1$, $m=20$, $\kappa=10$, and the quantization intervals are $\psi=1.8$ and $\psi=5$, respectively. The other parameters are the same as the first set of simulations. Fig.7 shows the simulation results for different quantization intervals. Fig.7(a)-(b) show that the quantization effect is better with $\psi=5$. From

TABLE IV
COMPARISON OF COMPUTATIONAL COMPLEXITY

Controller process	Complexity
The complexity of the new controller: $29O(1)+O(\log(n))$	
Designed parameters assignment: $\lambda,\eta,\xi_1,\xi_0,t_\xi$	$O(1)+O(1)+O(1)+O(1)+O(1)=5O(1)$
Error transformation: z	$O(1)$
Prescribed performance function: $\rho(t)$	$O(1)+O(1)=2O(1)$
Control law: $v(t)$	$O(1)$
Input quantizer: $Q_v(v)$	$14O(1)+O(\log(n))$
Event-triggering mechanism: $u(t)$	$3O(1)+3O(1)=6O(1)$
The complexity of the ETC [3]: $75O(1)+2O(n^2)+2O(n^3)$	
Designed parameters assignment: $t_k,\eta_1,\eta_2,\epsilon,\rho,\gamma_i,\sigma_i,i=1,2,3$	$11O(1)$
Error transformation: z_1,z_2	$4O(1)+O(1)=5O(1)$
Virtual control law: $\alpha(t)$	$O(1)$
Control law: v_c	$6O(1)$
Adaptive laws: $\theta,\hat{W},\hat{c}$	$3O(1)$
Event-triggering mechanism: $u(t)$	$3O(1)+3O(1)=6O(1)$
Type-2 fuzzy logic system: $\xi(x)$	$43O(1)+2O(n^2)+2O(n^3)$.

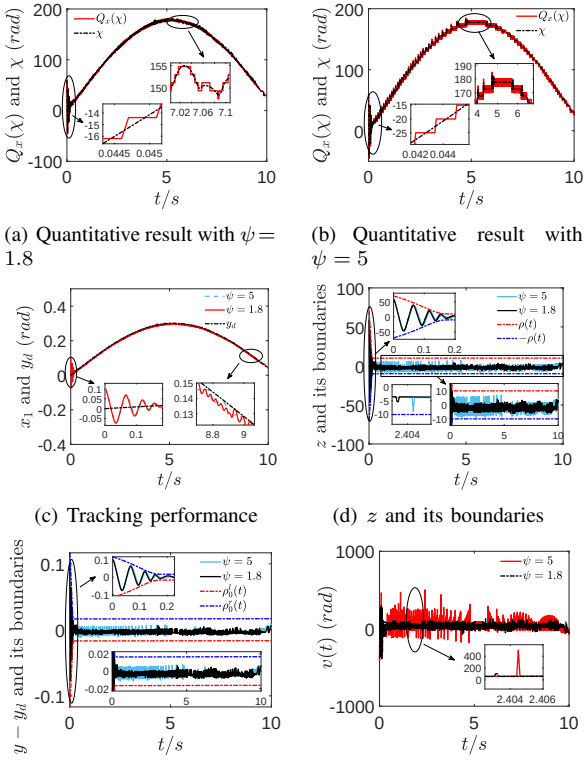

(a) Quantitative result with $\psi=1.8$
(b) Quantitative result with $\psi=5$
(c) Tracking performance
(d) z and its boundaries
(e) $y-y_d$ and its boundaries
(f) Control law $v(t)$

Fig. 7. Comparison of state quantization with different quantization interval.

Fig.7(c)-(f), it can be seen that within the same prescribed range of z, both controller can track the desired signal and the error $y-y_d$ is within the presetting boundary. However, for quantization interval $\psi=5$, control law jitter is more severe. Combined with (10) and (21), the main reason is that the z with $\psi=5$ is easier to approach the boundary, it will produce the larger control law. (ii) In this paper, the Big O notation is introduced to display the complexity of the algorithm, where n is the input of the algorithm and $O(1)<O(logn)<O(n)<O(nlogn)<O(n^2)<O(n^3)$. Tab.IV provides the comparison results of controller complexity. It can be seen that the $O(n^3)\gg O(\log(n))$, and the new controller has much lower computational complexity than ETC [3].

C. Experimental parameters selection

1) Experimental Platform: Fig.8 shows the automated vehicle experiment platform equipped with the SbW system, which includes a control unit (dSPACE-ds1202), the steering motor (XiNJE MS80ST-M02430B-20P7), a servo motor driver (XiNJE DS2-20P7), a linear sensor (KTR11-10). The experimental data is displayed and stored by a regular computer. The sampling time in the experiment is chosen as 0.001s. To simulate the effect of input nonlinearity on the control performance of SbW systems in the experiment, the control signal of SbW systems is simulated as $u_m=\ell(t)u+\varsigma(t)$, where u_m is the control signal transmitted to the actuator of SbW systems, and $\ell(t)$ and $\varsigma(t)$ chosen in the experiment are the same as those in the simulation.

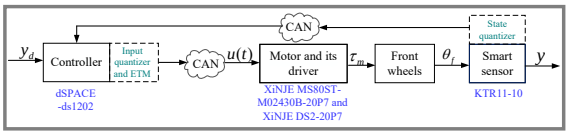

(a) Schematic diagram of the experiment platform with CAN being the Controller Area Network

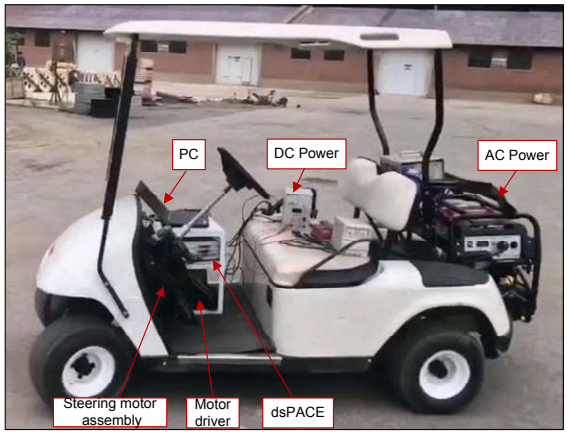

(b) Physical diagram of the experiment platform

Fig. 8. The experiment platform of SbW systems.

2) Controller parameters selection: In the experiment, the parameters of the designed control method (9)-(13) are chosen as $\lambda = 60$, $\eta = 60$, $\xi_0 = 12$, $\xi_1 = 0.8$, and the predetermined steady-state time $t_\xi = 0.5$. Finally, the desired signal is selected as $y_d = 0.4sin(0.4t)\ rad$, and the parameters of quantizers and event-triggering mechanism chosen in the experiment are the same as those in the simulation.

D. Experimental results and analysis

Fig.9 gives the control performance of SbW systems in the experiment under the control method designed in this paper. From Fig.9(a), it can be found that satisfactory tracking performance can be achieved under the designed control method. Fig.9(b)-Fig.9(e) show that the transformed error z, the tracking error $y - y_d$, and the states x_1 and x_2 can be constrained in the prescribed ranges. Fig.9(f)-Fig.9(g) give quantization results in the experiment under the state and input quantizer. It is easy to find that in the designed quantitative control system, both the state and input are well quantified. Fig.9(g) and Fig.9(h) show the results of the ETM output of the SbW system, and one can find that communication resources are saved by the ETM designed in this paper.

V. Conclusions

This paper addresses the problem of the low-complexity prescribed performance control for uncertain SbW systems with input nonlinearity, full-state constraints, and communication bandwidth limitations. Based on the new error transformation and barrier Lyapunov function technique, the model uncertainty, input nonlinearity, quantization, and event-triggering errors of the SbW system are handled, the tracking performance can be guaranteed. Besides, the dual quantization control

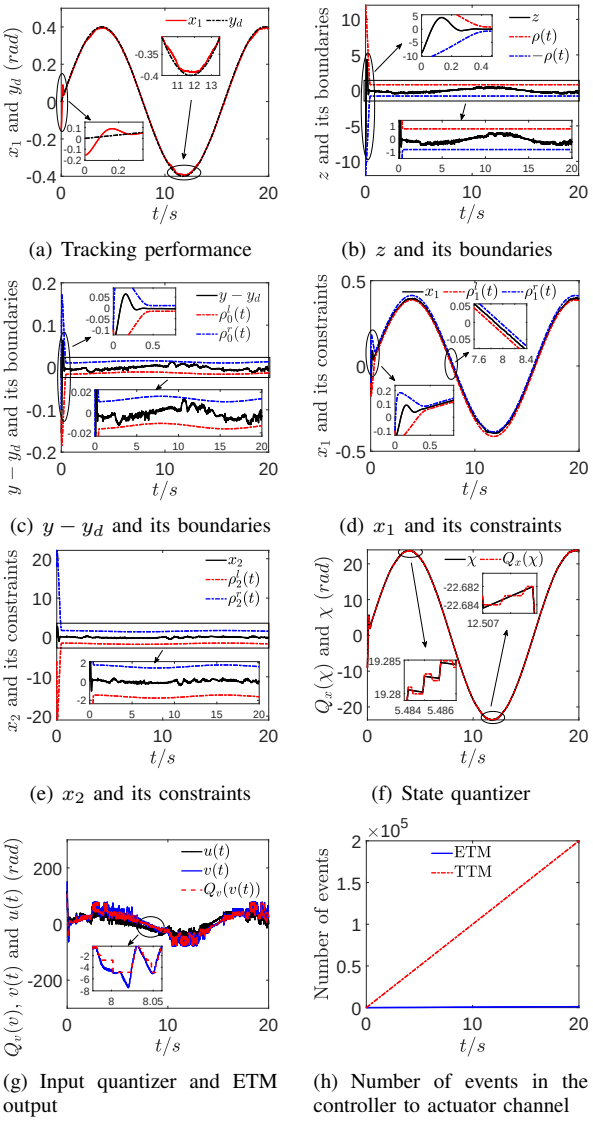

(a) Tracking performance

(b) z and its boundaries

(c) $y - y_d$ and its boundaries

(d) x_1 and its constraints

(e) x_2 and its constraints

(f) State quantizer

(g) Input quantizer and ETM output

(h) Number of events in the controller to actuator channel

Fig. 9. Control performance in experiment.

strategy developed effectively compensates for the effect of discontinuous signals caused by state and input quantization, and the communication bandwidth and energy consumption are saved. Itisnoteworthythat the full-state of SbW systems can be constrained, and communication resources can be saved. Theoretical analysis, simulation, and experiment are presented to verify the validity of the proposed control method. Future research will focus on solving the saturations of the control input rates and limitations of the actuator in SbW systems control.

Appendix A: Proof of *Lemma 2*

Proof: Combined with (9) and *Theorem 1*, one gets

$$-\rho(t) + \lambda y_d \leq \dot{x}_1 + \lambda x_1 \leq \rho(t) + \lambda y_d \tag{26}$$

$$(-\rho(t) + \lambda y_d)e^{\lambda t} \leq \frac{d}{dt}(x_1 e^{\lambda t}) \leq (\rho(t) + \lambda y_d)e^{\lambda t}. \tag{27}$$

Integrating (27), one has

$$e^{-\lambda t}\int_0^t(-\rho(t)+\lambda y_d)e^{\lambda t}dt+x_1(0)e^{-\lambda t}\le x_1 \le e^{-\lambda t}\int_0^t(\rho(t)+\lambda y_d)e^{\lambda t}dt+x_1(0)e^{-\lambda t}. \tag{28}$$

From (28), it can be concluded that the tracking error can converge to the prescribed neighborhood of the origin, i.e.,

$$e^{-\lambda t}\int_0^t(-\rho(t)+\lambda y_d)e^{\lambda t}dt+x_1(0)e^{-\lambda t}-y_d\le x_1-y_d \le e^{-\lambda t}\int_0^t(\rho(t)+\lambda y_d)e^{\lambda t}dt+x_1(0)e^{-\lambda t}-y_d. \tag{29}$$

Combined with (26) and (29), one gets

$$-\rho(t)-\lambda\left(e^{-\lambda t}\int_0^t(\rho(t)+\lambda y_d)e^{\lambda t}dt+x_1(0)e^{-\lambda t}-y_d\right)\le x_2 \le\rho(t)-\lambda\left(e^{-\lambda t}\int_0^t(-\rho(t)+\lambda y_d)e^{\lambda t}dt+x_1(0)e^{-\lambda t}-y_d\right). \tag{30}$$

Combining (28), (29), (30) and the bounds of $x_1(0)$, one gets

$$\rho_0^l\le x_1-y_d\le\rho_0^r,\ \rho_i^l\le x_i\le\rho_i^r,\quad i=1,2 \tag{31}$$

with $\rho_i^l(t)$, $\rho_i^r(t)$, $i=0,1,2$, $\rho_i^l(t)$ and $\rho_i^r(t)$ being defined as $\rho_1^l(t)=e^{-\lambda t}\int_0^t(-\rho(t)+\lambda y_d)e^{\lambda t}dt+x_1(0)e^{-\lambda t}$, $\rho_1^r(t)=e^{-\lambda t}\int_0^t(\rho(t)+\lambda y_d)e^{\lambda t}dt+x_1(0)e^{-\lambda t}$, $\rho_2^l(t)=-\rho(t)-\lambda\rho_1^r(t)$, $\rho_2^r(t)=\rho(t)-\lambda\rho_1^l(t)$, $\rho_0^l(t)=\rho_1^l(t)-y_d$, and $\rho_0^r(t)=\rho_1^r(t)-y_d$.

This ends the proof of *Lemma 2*. ■

APPENDIX B: DERIVATIONS OF τ_e

According to existing research [34], the self-aligning torque τ_e can be expressed as

$$\tau_e=(t_m+t_p)(F_{yfl}+F_{yfr}), \tag{32}$$

where $F_{yi}, i=fl,fr$, means the front tyre forces in the y direction, is usually difficult to measure in practical applications, which can be related to the tyres lateral force F_{ti} and tractive force F_{si} as

$$F_{yi}=F_{ti}\sin\theta_i+F_{si}\cos\theta_i, \tag{33}$$

where $\theta_i=\theta+k_{rsf}\phi$ with k_{rsf} being the front roll steer coefficient and ϕ being the roll angle, the tyres lateral force $F_{ti}$and tractive force F_{si} are modeled as

$$F_{ti}=\frac{C_{s_i}s_{\omega_i}}{1-s_{\omega_i}}\Gamma(\delta_i), F_{si}=\frac{C_{\alpha_i}\tan\alpha_i}{1-s_{\omega_i}}\Gamma(\delta_i), \tag{34}$$

where C_{si} and $C_{\alpha i}$ are the longitudinal stiffness and cornering stiffness of each front tyre, and

$$\Gamma(\delta_i)=\begin{cases}\delta_i(2-\delta_i), if 0\le\delta_i<1\\ 1, otherwise\end{cases}, \tag{35}$$

$$\delta_i=\frac{\mu(t)F_{zi}\left(1-\varepsilon_r v_{ti}\sqrt{s_{\omega_i}^2+\tan^2\alpha_i}\right)(1-s_{\omega_i})}{2\sqrt{C_{\omega_i}^2s_{\omega_i}^2+C_{\alpha_i}^2\tan^2\alpha_i}}, \tag{36}$$

with $\mu(t)$, $0\le\mu(t)\le1$, being the time-varying friction coefficient between the tyre and the ground, F_{zi} is the normal load on the tyre, ε_r being the road adhesion reduction factor, and the sliding rate of each front tyre $s_{\omega i}$, $0\le s_{\omega i}\le1$, being defined as

$$s_{\omega_i}=\frac{\max(v_{ti},\omega_i r)-\min(v_{ti},\omega_i r)}{\max(v_{ti},\omega_i r)}, \tag{37}$$

where v_{ti} is the front wheel centre speed in the direction of the tyre heading and can be written for each front wheel as

$$v_{tfl}=(v_x+\frac{1}{2}d_f\gamma)\cos\theta_f+(v_y+l_f\gamma)\sin\theta_f, \tag{38}$$

$$v_{tfr}=(v_x-\frac{1}{2}d_f\gamma)\cos\theta_f+(v_y+l_f\gamma)\sin\theta_f, \tag{39}$$

where v_x, v_y and γ are the vehicles longitudinal velocity, lateral velocity and yaw rate, respectively. The slip angles of the front wheels are

$$\alpha_{fl}=\theta_{fl}-\arctan\left(\frac{v_y+l_f\gamma}{v_x-d_f\gamma/2}\right), \tag{40}$$

$$\alpha_{fl}=\theta_{fr}-\arctan\left(\frac{v_y+l_f\gamma}{v_x+d_f\gamma/2}\right). \tag{41}$$

Reference [34] provides detailed derivation and parameter definitions.

REFERENCES

[1] L. He, F. Li, C. Guo, B. Gao, J. Lu, and Q. Shi, "An adaptive pi controller by particle swarm optimization for angle tracking of steer-by-wire," *IEEE/ASME Transactions on Mechatronics*, vol. 27, no. 5, pp. 3830–3840, 2022.

[2] C. Huang, F. Naghdy, and H. Du, "Observer-based fault-tolerant controller for uncertain steer-by-wire systems using the delta operator," *IEEE/ASME Transactions on Mechatronics*, vol. 23, no. 6, pp. 2587–2598, 2018.

[3] Y. Wang, B. Ma, D. Wang, and T. Chai, "Event-triggered prespecified performance control for steer-by-wire systems with input nonlinearity," *IEEE Transactions on Intelligent Transportation Systems*, vol. 24, no. 7, pp. 6922–6931, 2023.

[4] X. Wu, M. Zhang, and M. Xu, "Active tracking control for steer-by-wire system with disturbance observer," *IEEE Transactions on Vehicular Technology*, vol. 68, no. 6, pp. 5483–5493, 2019.

[5] B. Ma, Y. Wang, and T. Chai, "Event-triggered output feedback type-2 fuzzy control for uncertain steer-by-wire systems with prespecified tracking performance," *IEEE Transactions on Fuzzy Systems*, vol. 30, no. 8, pp. 3098–3112, 2022.

[6] B. Ma and Y. Wang, "Adaptive output feedback control of steer-by-wire systems with event-triggered communication," *IEEE/ASME Transactions on Mechatronics*, vol. 26, no. 4, pp. 1968–1979, 2021.

[7] H. Wang, H. Kong, Z. Man, D. M. Tuan, Z. Cao, and W. Shen, "Sliding mode control for steer-by-wire systems with ac motors in road vehicles," *IEEE Transactions on Industrial Electronics*, vol. 61, no. 3, pp. 1596–1611, 2014.

[8] M. Do, Z. Man, C. Zhang, H. Wang, and F. Tay, Tay, "Robust sliding mode-based learning control for steer-by-wire systems in modern vehicles," *IEEE Transactions on Vehicular Technology*, vol. 63, no. 2, pp. 580–590, 2014.

[9] H. Wang, Z. Man, W. Shen, Z. Cao, J. Zheng, J. Jin, and D. M. Tuan, "Robust control for steer-by-wire systems with partially known dynamics," *IEEE Transactions on Industrial Informatics*, vol. 10, no. 4, pp. 2003–2015, 2014.

[10] C. Huang, F. Naghdy, and H. Du, "Delta operator-based fault estimation and fault-tolerant model predictive control for steer-by-wire systems," *IEEE Transactions on Control Systems Technology*, vol. 26, no. 5, pp. 1810–1817, 2018.

[11] M. B. N. Shah, A. R. Husain, H. Aysan, S. Punnekkat, R. Dobrin, and F. A. Bender, "Error handling algorithm and probabilistic analysis under fault for can-based steer-by-wire system," *IEEE Transactions on Industrial Informatics*, vol. 12, no. 3, pp. 1017–1034, 2016.
[12] C. Huang, F. Naghdy, and H. Du, "Fault tolerant sliding mode predictive control for uncertain steer-by-wire system," *IEEE Transactions on Cybernetics*, vol. 49, no. 1, pp. 1810–1817, 2019.
[13] Y. Wang, Y. Liu, Y. Wang, and T. Chai, "Neural output feedback control of automobile steer-by-wire system with predefined performance and composite learning," *IEEE Transactions on Vehicular Technology*, vol. 72, no. 5, pp. 5906–5921, 2023.
[14] S. Gao, M. Li, Y. Zheng, and H. Dong, "Expansive errors-based fuzzy adaptive prescribed performance control by residual approximation," *IEEE Transactions on Fuzzy Systems*, vol. 30, no. 7, pp. 2736–2746, 2022.
[15] J.-X. Zhang and T. Chai, "Singularity-free continuous adaptive control of uncertain underactuated surface vessels with prescribed performance," *IEEE Transactions on Systems, Man, and Cybernetics: Systems*, vol. 52, no. 9, pp. 5646–5655, 2022.
[16] S. Sui, C. L. P. Chen, and S. Tong, "A novel full errors fixed-time control for constraint nonlinear systems," *IEEE Transactions on Automatic Control*, vol. 68, no. 4, pp. 2568–2575, 2023.
[17] Y.-J. Liu, Q. Zeng, S. Tong, C. L. P. Chen, and L. Liu, "Actuator failure compensation-based adaptive control of active suspension systems with prescribed performance," *IEEE Transactions on Industrial Electronics*, vol. 67, no. 8, pp. 7044–7053, 2020.
[18] Z. Gao, Y. Zhang, and G. Guo, "Fixed-time prescribed performance adaptive fixed-time sliding mode control for vehicular platoons with actuator saturation," *IEEE Transactions on Intelligent Transportation Systems*, vol. 23, no. 12, pp. 24 176–24 189, 2022.
[19] L. Zhang and G.-H. Yang, "Adaptive fuzzy prescribed performance control of nonlinear systems with hysteretic actuator nonlinearity and faults," *IEEE Transactions on Systems, Man, and Cybernetics: Systems*, vol. 48, no. 12, pp. 2349–2358, 2018.
[20] Z. Gao, Y. Zhang, and G. Guo, "Finite-time fault-tolerant prescribed performance control of connected vehicles with actuator saturation," *IEEE Transactions on Vehicular Technology*, vol. 72, no. 2, pp. 1438–1448, 2023.
[21] Z. Wang, H.-K. Lam, Y. Guo, B. Xiao, Y. Li, X. Su, E. M. Yeatman, and E. Burdet, "Adaptive event-triggered control for nonlinear systems with asymmetric state constraints: A prescribed-time approach," *IEEE Transactions on Automatic Control*, vol. 68, no. 6, pp. 3625–3632, 2023.
[22] Y. Cao, J. Cao, and Y. Song, "Practical prescribed time control of eulerlagrange systems with partial/full state constraints: A settling time regulator-based approach," *IEEE Transactions on Cybernetics*, vol. 52, no. 12, pp. 13 096–13 105, 2022.
[23] L. Shen, H. Wang, and H. Yue, "Prescribed performance adaptive fuzzy control for affine nonlinear systems with state constraints," *IEEE Transactions on Fuzzy Systems*, vol. 30, no. 12, pp. 5351–5360, 2022.
[24] C. Hua, P. Ning, K. Li, and X. Guan, "Fixed-time prescribed tracking control for stochastic nonlinear systems with unknown measurement sensitivity," *IEEE Transactions on Cybernetics*, vol. 52, no. 5, pp. 3722–3732, 2022.
[25] Y. Gao, J. Liu, Z. Wang, and L. Wu, "Interval type-2 fnn-based quantized tracking control for hypersonic flight vehicles with prescribed performance," *IEEE Transactions on Systems*, vol. 51, no. 3, pp. 1981–1993, 2019.
[26] L. N. Bikas and G. A. Rovithakis, "Combining prescribed tracking performance and controller simplicity for a class of uncertain mimo nonlinear systems with input quantization," *IEEE Transactions on Automatic Control*, vol. 64, no. 3, pp. 1228–1235, 2019.
[27] J.-X. Zhang and G.-H. Yang, "Fault-tolerant output-constrained control of unknown euler-lagrange systems with prescribed tracking accuracy," *Automatica*, vol. 111, p. 108606, 2020.
[28] L. N. Bikas and G. A. Rovithakis, "Prescribed performance tracking of uncertain mimo nonlinear systems in the presence of delays," *IEEE Transactions on Automatic Control*, vol. 68, no. 1, pp. 96–107, 2023.
[29] J.-X. Zhang and G.-H. Yang, "Low-complexity tracking control of strict-feedback systems with unknown control directions," *IEEE Transactions on Automatic Control*, vol. 64, no. 12, pp. 5175–5182, 2019.
[30] H. Wang, Z. Man, H. Kong, Y. Zhao, M. Yu, Z. Cao, J. Zheng, and M. Do, "Design and implementation of adaptive terminal sliding mode control on a steer-by-wire equipped road vehicle," *IEEE Transactions on Industrial Electronics*, vol. 63, no. 9, pp. 5774–5785, 2016.
[31] J. Zhou, C. Wen, W. Wang, and F. Yang, "Adaptive backstepping control of nonlinear uncertain systems with quantized states," *IEEE Transactions on Automatic Control*, vol. 64, no. 11, pp. 4756–4763, 2019.
[32] Y.-H. Jing and G.-H. Yang, "Fuzzy adaptive quantized fault-tolerant control of strict-feedback nonlinear systems with mismatched external disturbances," *IEEE Transactions on Systems, Man, and Cybernetics: Systems*, vol. 50, no. 9, pp. 3424–3434, 2020.
[33] Z. Sun, J. Zheng, Z. Man, and H. Wang, "Robust control of a vehicle steer-by-wire system using adaptive sliding mode," *IEEE Transactions on Industrial Electronics*, vol. 63, no. 4, pp. 2251–2262, 2016.
[34] H. Du, J. Lam, K.-C. Cheung, W. Li, and N. Zhang, "Side-slip angle estimation and stability control for a vehicle with a non-linear tyre model and a varying speed," *Proceedings of The Institution of Mechanical Engineers Part D-journal of Automobile Engineering*, vol. 229, no. 4, pp. 486–505, 2015.

Jiwu Li is currently working toward the M.S. degree in vehicle engineering at Yanshan University, Qinhuangdao, China. His current research interests include robust and prescribed performance control control of nonlinear electromechanical systems.

Bingxin Ma received the Ph.D. degree in mechanical engineering and automation from Northeastern University, Shenyang, China, in 2022. He is currently a lecturer with the School of Vehicle and Energy, Yanshan University and Hebei Key Laboratory of Special Carrier Equipment, Qinhuangdao, China. His research interests include intelligent modeling and robust control of nonlinear systems.

Hongjuan Li is currently working toward the Ph.D. degree at the School of Mechanical Engineering and Automation, Northeastern University, Shenyang, China. Her research interests include intelligent modeling and control of steer-by-wire systems.

Yongfu Wang received the Ph.D. degree in control science and engineering from Northeastern University, Shenyang, China, in 2005. He is currently a Professor with the School of Mechanical Engineering and Automation, Northeastern University, Shenyang, China. His research interests include intelligent modeling and adaptive control of nonlinear systems.